Philosophical Magazine
First published in 1798

Phase diagrams of decomposing nanoalloys

A. S. Shirinyan [a]; A. M. Gusak [a]

[a] Department of Physics, Cherkasy B. Khmelnytsky National University. Cherkasy 18017. Ukraine

PLEASE SCROLL DOWN FOR ARTICLE

Phase diagrams of decomposing nanoalloys

A. S. Shirinyan† and A. M. Gusak‡

Department of Physics, Cherkasy B. Khmelnytsky National University,
81 Shevchenko Street, Cherkasy 18017, Ukraine

Abstract

The thermodynamics of nucleation and decomposition in small isolated particles are considered. There exist three possibilities: phase separation, prohibition of decomposition and a metastable state. We investigate the peculiarities of phase diagrams related to depletion of the nanosize parent phase even at the nucleation stage. For small particles the equilibrium diagram becomes split (and shifted and size dependent). Concentration, size and temperature hystereses take place. Size-dependent 'critical supersaturation', increasing with decreasing size, has been analysed.

§ 1. Introduction

All stages of decomposition of a supersaturated binary alloy (a parent phase containing A and B components) with precipitation of an intermediate phase 1 have been extensively studied in the case of a macroscopic sample size (Christian 1965). In the first two stages, namely the nucleation and growth of precipitates, the depletion of the matrix (change in the average concentration) is usually neglected. It becomes crucial in the last stage: ripening (Lifshits and Slezov 1961, Wagner 1961). Thus a description of the first two stages is based on the driving forces and equilibrium boundary concentrations for bulk macroscopic materials. If the decomposition develops from the viewpoint of nanometric volumes, then the size effect comes into play (Palatnik and Comnik 1960, Denbigh and Marcus 1966, Hutchinson 1963). The phase diagram of nanosize systems is an urgent issue for nanoelectronics, thin film technologies, nucleation in atmospheric aerosols, etc.

A theoretical description of size effects is usually based on two basic factors:

 (i) the increase in excess surface energy per atom of a small particle (Petrov 1982, Nagaev 1992)
 (ii) the change in vacancy concentration (for example Gladgkikh *et al.* (1988) and Wautelet (1991).

Yet, there exists one more fundamental reason for the size effect in a binary (or multicomponent) alloy, where the first-order phase transformation includes a change in composition (Rusanov 1967, Ulbricht *et al.* 1988). Indeed, such a transformation should start from nucleation, but the amount of one of the components

† Author for correspondence. Email: shirinyan@phys.cdu.edu.ua.
‡ Email: gusak@univer.cherkassy.ua.

in the whole particle may not be enough for the construction of a critical nucleus. In other words, when the new phase crystal nucleates in a small particle, depletion of the surrounding parent phase may occur. The effect of depletion of the parent phase on nucleation and growth in nanovolumes cannot be neglected (Ludwig and Schmelzer 1996) (see also Gusak and Shirinyan (1998)). It has been found that the driving forces and nucleation barriers depend on the size of decomposing particles (caused by the above-mentioned depletion). A change in density may have the same effect in one-component systems as a change in composition (see, in particular, Schmelzer and Schweitzer (1990)). Yet, the peculiarities of phase diagrams for nano-systems have not been sufficiently studied. For example, the very notion of phase diagram changes since the first stage of decomposition in small particle could also be simultaneously the last stage.

Experimental results on the effect of size on phase transformations in alloys have been obtained in a few studies (for example Gladgkikh *et al.* (1988)). Investigation of the phase equilibrium in thin binary Bi–Sn (eutectic) and Bi–Pb (eutectic and peritectic) films demonstrated a decrease in the eutectic temperature by 5, 10 and 18 K for the respective film thicknesses 32, 20 and 10 nm. In general, a decrease in liquidus and solidus lines was observable for thickness of less than 50 nm. Simplified theoretical analysis (Wautelet 2000) resulted in the same effect: a decreasing lens-type liquidus–solidus diagram with decreasing size. On the other hand, the opposite behaviour, namely increasing melting temperature for decreasing size, has been reported for Pb particles in Al (for example Moore *et al.* (1987)).

Size effect can also lead to a change in the solubilities in the solid state. For example, the limit solubility of Cu in Ag was 6 at.% for a 27 nm film and 15–17 at.% for a 7 nm film. (These metals have only a fcc lattice. So this is not the case of poly-morphic transitions under the size effect.) Therefore, for bulk alloys the limit value of Cu solubility in Ag is 0.35 at.% (Chighik *et al.* 1985) for the same temperature ($20°C$).

The main purpose of the present paper is to describe the fundamental differences between the phase diagrams for bulk materials and nanomaterials, related to the finite (non-negligible) depletion of nanoparticles even at the nucleation stage. To achieve this aim, we should first formulate the basic equations for the thermody-namics of decomposition in small particles and then apply them to the model alloy. In §2 we describe a simplified model system. In §3 we briefly formulate the main results for the Gibbs energy versus size dependences. In §4 we discuss the size effect for the temperature of phase separation. In §5 we concentrate on the peculiarities of the size-dependent phase diagram, introducing the notions of equilibrium curve splitting, critical supersaturation and hysteresis. In appendix A we illustrate the hysteresis phenomenon in small particles in the framework of the simplified master equation approach.

§2. MODEL

A very naive illustration of the essence of the size effect related to parent phase depletion is as follows. If the nucleus of the new phase 1 of radius r^* with mole fraction X_1 of species B is formed in a parent phase with a much lower initial mole fraction X_0, it should 'suck out' the atoms B from the sphere (supply region) with a radius not less than $R^* = (X_1 v_1 / X_0 v)^{1/3} r^*$ (here v and v_1 are the volumes per atom in the parent and new phases respectively). Obviously, if the size of the whole particle is less than the above-mentioned value R, and r^* is the critical size of nucleus in bulk material, nucleation becomes impossible; the total number of atoms B in the whole

particle is just not sufficient for the construction of even a single stable nucleus. Taking $r^* = 10^{-9}$ m, $X_0 = 0.1$, $v/v_1 \approx 1$ and $X_1 = 0.8$, one obtains for the 'minimal' radius R^* of the supply region $R^* = 2$ nm. When $R < 2$ nm, nucleation is absolutely impossible. In fact, this is only an estimation since, on depletion of the parent phase with, say, atoms B, the Gibbs free energy increases owing to the decrease in entropy. Therefore, nucleation becomes impossible already for some particle size $R > R^*$. To obtain quantitative results, we should choose the thermodynamic models for the new and parent phases.

Let us choose the model of the new phase as a 'line' (strictly stoichiometric) intermediate phase and exclude the elastic contributions to the Gibbs energy. We shall consider the formation of a spherical nucleus of intermediate phase inside the spherical particle of supersaturated solid solution at initial concentration X_0 (figure 1).

Of course, nucleation can proceed well at the external boundary (the 'cap' of new phase). This case has been treated elsewhere (Shirinyan 2000). We shall not discuss the corresponding results here since they are basically the same and differ from the present model only quantitatively.

According to the simplified model presented here, at any moment and at any size r (radius) of the growing nucleus, the mole fraction distribution is assumed to be step like (without transient layers) so that the concentration is uniform inside each phase (see §6).
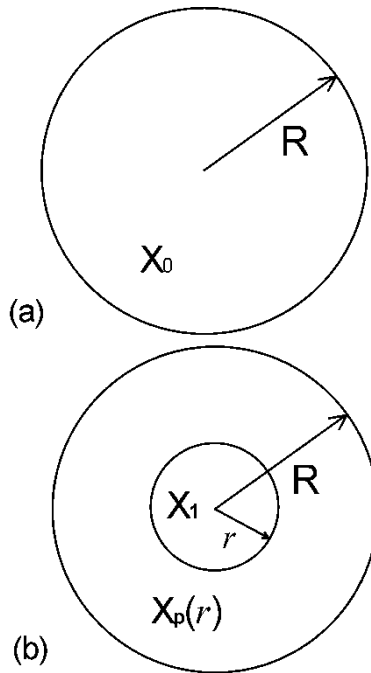
Figure 1. Schematic representation of phase transformation: (a) particle of concentration X_0 before transformation; (b) the same particle after the transformation with concentration redistribution being taken into account. $X_p(r)$ is the concentration of the ambient parent phase, X_1 the concentration of strong stochiometric intermediate phase, r the nucleus size and R the radius of the supply region (nanometric isolated particle).

We suppose that, for any given nucleus size r, the mole fractions X_1 and X_p of species B in the new and parent phases respectively satisfy the condition of minimum Gibbs free energy. The mole fractions are related by the following evident conservation law:

$$nX_0V_0 = n_1X_1V_1 + nX_pV_p, \qquad (1)$$

where X_0 is the mole fraction before nucleation, V_1 is the volume of the new models formed, and V_0 and V_p are the volumes of the parent phase before transformation and after nucleation respectively. In the following, the numbers n of atoms per unit volume are taken the same for old and new phases ($n_1 = n$). For spherically symmetric clusters the volumes of the phases are as follows:

$$V_1 = \tfrac{4}{3}\pi r^3, \qquad V_p = \tfrac{4}{3}\pi(R^3 - r^3), \qquad V_0 = \tfrac{4}{3}\pi R^3.$$

Depletion of the remaining parent phase ($\Delta X \equiv X_0 - X_p$) is a function of the nucleus size r, radius R and mean concentrations X_0 and X_1: $\Delta X(r) = (X_1 - X_0)\,r^3/(R^3 - r^3)$. For the case $X_1 > X_0$ presented here, one obtains $X_p(r) < X_0$ (depletion of matrix by the B component).

The Gibbs energy per atom of the new phase 1 (line compound) and of the parent phase are taken as (figure 2)

$$\Delta g_1(T) = \Delta g_1 + \alpha kT \quad (X = X_1), \qquad (2)$$

$$\Delta g_0(T, X) = kT[X\ln(X) + (1 - X)\ln(1 - X)]. \qquad (3)$$

Here Δg_1 is the isothermal Gibbs energy of formation (per atom) from pure solid components, $\alpha > 0$ is a non-dimensional parameter determining the temperature-dependent behaviour of the driving force and k is the Boltzmann constant.
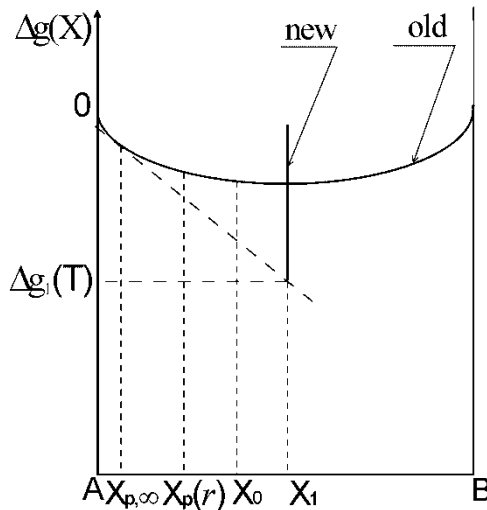
Figure 2. The Gibbs free energy $\Delta g(X)$ (per atom) as a function of concentration for the 'old' (parent) and 'new' (phase 1) phases (qualitative dependence). X_0 is the initial concentration of the parent phase, $X_p(r)$ is the concentration of the parent phase as a result of fluctuation, nucleation and/or separation, $X_{p,\infty}$ is the equilibrium concentration in the parent phase corresponding to the full separation in an infinite matrix. (In this diagram the pure components are assumed to have the same structures.)

The linear approximation for $\Delta g_1(T)$ corresponds to the experimental situation and is commonly used (for example Chen *et al.* (1989) and Saunders (1977)). Equation (3) corresponds to the ideal solution. In fact, a model of regular solution would be more reasonable since the existence of the intermediate phases usually correlates with a negative mixing energy. However, for simplicity, below we restrict ourselves to the case of negligible mixing energy. The influence of the deviation from an ideal solution will be analysed in detail elsewhere.

Usually increasing the temperature yields a decrease in the bulk driving force. So we adjust the parameter α in equation (2) to satisfy the condition

$$\Delta g_0(T_\infty, X_0) + \left.\frac{\partial[\Delta g_0(T_\infty, X)]}{\partial X}\right|_{X_0} (X_1 - X_0) = \Delta g_1(T_\infty)$$

at a characteristic temperature T_∞ (the separation temperature in an infinite matrix) and concentration $X_0 = X_{p,\infty}$ (the solubility in an infinite matrix).

The expression for the change in the Gibbs free energy after nucleation of the phase 1 nucleus of radius r is

$$\Delta G = nV_1 \Delta g_1(T) + nV_p \Delta g_0\big(T, X_p(r)\big) - nV_0 \Delta g_0(T, X_0) + 4\pi r^2 \sigma. \qquad (4)$$

In equation (4) again the numbers n of atoms per unit volume are taken to be the same in the two phases ($V_p = V_0 - V_1$; $V_0 = 4\pi R^3/3$) and the surface interphase tension σ is taken to be independent of the temperature T (Wautelet 2000).

The extremes of the ΔG function in equation (4) have been found by direct calculation of ΔG for all reasonable sizes r (with a small step).

§3. Thermodynamic equilibrium analysis in small particles

Let us plot the Gibbs free energy versus the nucleus size $\Delta G(r)$ according to equation (4) for different temperatures, initial concentrations X_0 and particle sizes. The typical schematic dependences are presented in figure 3 (for example Ulbricht *et al.* (1988), Ludwig and Schmelzer (1996) and Gusak and Shirinyan (1998)).

One can obtain the spectrum of all states by changing the initial supersaturation (due to the composition and temperature) and the size of the transforming particle. Therefore, possible cases are separation (cases T_3, R_3 and X_{03} in figure 3), a meta-stable state (cases T_2, R_2 and X_{02} in figure 3) and the impossibility of separation (cases T_1, R_1 and X_{01} in figure 3). The last situation for a small particle may be realized even at concentrations and temperatures for which separation is possible in an infinite alloy.

§4. Influence of decreasing size on the phase transformation (separation) temperature

To verify whether our model is reasonable, let us consider the influence of decreasing size on the phase transformation temperature at a fixed initial composition and fixed particle size. This problem has been investigated earlier (Ulbricht *et al.* 1988), and a decrease in the transformation temperature with decreasing size was demonstrated. The transformation temperature was introduced by these workers traditionally as the critical temperature corresponding to simultaneous zero values of the first and second derivatives in the $\Delta G(r)$ dependence. Our criterion for transformation is different.
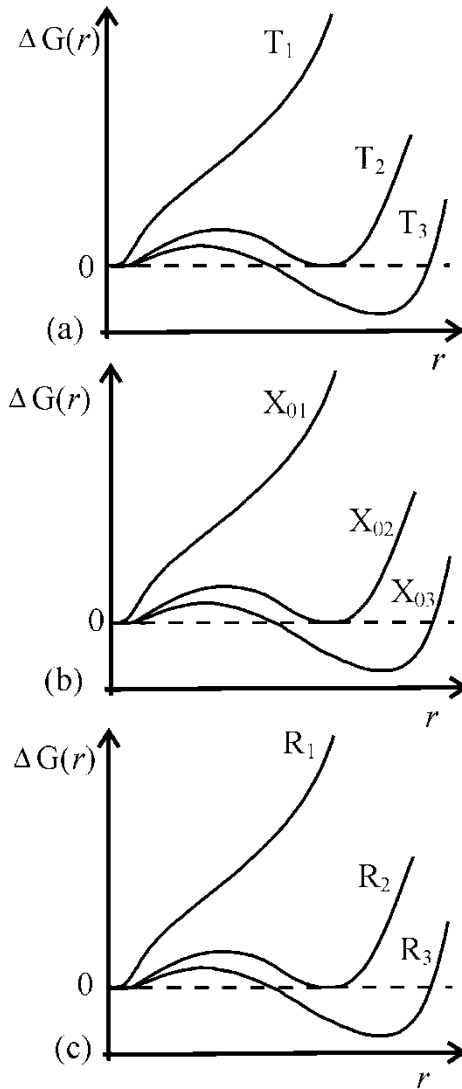
Figure 3.   Schematic Gibbs free-energy ΔG dependence on the radius r of the nucleus (a) for different temperatures $T_1 > T_2 > T_3$ and other fixed parameters, (b) for different initial concentrations X_0 ($X_{01} < X_{02} < X_{03}$), provided that other parameters are fixed and (c) for different radii of the particle ($R_1 < R_2 < R_3$). The graphs for T_2, R_2 and X_{02} (middles) correspond to the separation criterion.

We define the separation temperature T_{tr} as the temperature at which the dependence of the Gibbs free energy on the radius of the new phase becomes non-monotonic with a maximum and a zero second minimum: $\Delta G = 0$, $[\partial(\Delta G)/\partial r]|_R = 0$ for $r > 0$ (case T_2 in figure 3). This criterion will be further called the separation criterion. It seems more natural to us than the criterion of zero first and second derivatives. Note that the possibility of such a phase transition criterion has also been indicated by Schmelzer and Schweitzer (1990). The second minimum in the $\Delta G(r)$ dependence (the first is at $r = 0$) corresponds to the two-phase state: parent phase + phase 1 (figure 1 (b)). At typical values for intermetallic systems ($X_0 = 0.3$,
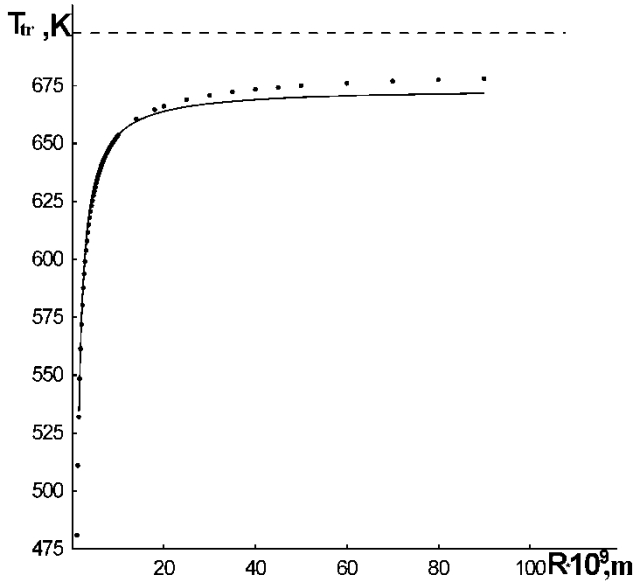
Figure 4. The separation temperature T_{tr} dependence versus the size of the decomposing particle. The horizontal broken line characterizes the separation temperature in an infinite matrix ($T_{\infty} = 698\,\mathrm{K}$). The full circles show the results of the Gibbs free-energy analysis in a small particle at the separation condition: $\Delta G = 0$, $[\partial(\Delta G)/\partial r]|_R = 0$, $r > 0$. The solid curve is the approximation function $T_{\mathrm{tr}} \approx T_{\infty}(\alpha + \beta/R)$, where $\alpha = 0.9656$ and $\beta = -2.894 \times 10^{-10}\,\mathrm{m}$. Explanations and parameters are in the main text. For example, at $R = 7 \times 10^{-9}\,\mathrm{m}$ (and the same set of parameters) it yields $T_{\mathrm{tr}} = 644\,\mathrm{K}$.

$n = 7 \times 10^{28}\,\mathrm{m}^{-3}$, $\sigma = 0.15\,\mathrm{Jm}^{-2}$, $\Delta g_1 = -3 \times 10^{-20}\,\mathrm{J}$, $X_1 = 0.5$ and $\alpha = 2.4$) the result of such analysis is presented in figure 4.

Note that the equilibrium condition in a small particle means equal depths of two pits (in the Gibbs free-energy dependence on the radius r), which are separated by a thermodynamic barrier. In the case of a small particle this barrier is of the order of the nucleation barrier and may not be high (less than $50\,kT$). This means that the phase equilibrium in an ensemble of small particles will correspond to a statistical distribution at which some particles will be in a single-phase state and the others in a two-phase state. The corresponding kinetic analysis has been given elsewhere (Schmelzer and Schweitzer 1990, Shirinyan 2000).

§5. INFLUENCE OF THE SIZE ON THE SOLUBILITY X_0

First of all we shall find the equilibrium concentration $X_{\mathrm{p},\infty} \equiv X_{\mathrm{p}}(R \to \infty)$ in the parent phase corresponding to the full separation in an infinite matrix (at every fixed temperature T). The second equilibrium concentration is equal to X_1 (which is known). The condition for optimal concentration $X_{\mathrm{p},\infty}$ and solubility limit X_0 can be found according to the common tangent rule:

$$\Delta g_0(T, X_{\mathrm{p},\infty}) + \left.\frac{\partial[\Delta g_0(T, X)]}{\partial X}\right|_{X_{\mathrm{p},\infty}} (X_1 - X_{\mathrm{p},\infty}) = \Delta g_1(T),$$

which is the transcendental equation in our case. For the case when $X_1 = 0.5$ (which we shall consider below) after easy algebra this transcendental equation may be

rewritten as a quadratic equation and it has the root

$$X_{p,\infty} = 0.5\left(1 - \left\{1 - 4\exp\left[2\left(\frac{\Delta g_1}{kT} + \alpha\right)\right]\right\}^{1/2}\right).$$

The second root

$$X_{p,\infty} = 0.5\left(1 + \left\{1 - 4\exp\left[2\left(\frac{\Delta g_1}{kT} + \alpha\right)\right]\right\}^{1/2}\right)$$

appears because of symmetry of the problem with respect to $X_1 = 0.5$ and corresponds to initial concentration $X_0 > 0.5$; so we do not consider this further. The cupola-shaped separation diagram T–X for an infinite matrix shifted towards a strong stoichiometric phase is presented below.

Let us take the radius of our binary system as $R = 10^{-8}$ m (at the same fixed parameters $n = 7 \times 10^{28}$ m^{-3}, $\sigma = 0.15$ J m^{-2}, $\Delta g_1 = -3 \times 10^{-20}$ J, $X_1 = 0.5$ and $\alpha = 2.4$). According to the separation criterion for a small particle (case X_{02} in figure 3), one can find the optimal concentration X_p^{opt} ($\equiv X_p^{opt}(R, T)$) of the parent phase corresponding to stable $\Delta G(r)$ minimum. Thus, we have two limiting points (the third meeting point, $X_1 = 0.5$, is determined from the initial condition) for the chosen criterion: the initial concentration $X_0^{cr}(R, T)$ (hereafter called X_0^{cr}) as the limit solubility of one component in another (B in A) and the optimal concentration X_p^{opt} of the depleted ambient parent phase as the result of separation. The size-dependent separation diagram is presented in figure 5 (case MQZNL).

Consider the influence of sizes on the solubility X_0^{cr} change at fixed temperature T_S ($T_S = T_Z$ in figure 5) and the above-cited parameters. The solubility X_0^{cr} in a bulk alloy is determined by the point X_S in figure 5, and in a small particle by the point X_Z ($X_Z > X_S$). For example, at $T_S = 680$ K the solubility X_0^{cr} in a bulk alloy will be $X_S = 6.4$ at.% and in a small particle ($R = 10^{-8}$ m) it will be $X_Z = 43$ at.%.

In other words, the bulk alloy in the concentration interval $X_0 < X_S$ will be thermodynamically stable with respect to separation. In the $X_S < X_0 < X_1$ interval the bulk alloy is unstable; it will be separated into a new phase of concentration X_1 and parent phase of concentration X_S.

The small particle with the same initial concentration X_0 ($X_0 < X_Z$) will not be separated, but the particle with the concentration $X_Z < X_0 < X_1$ will be separated into a new phase of concentration X_1 and a parent phase of concentration that is determined by the corresponding point of series DQ$'$E in figure 5 (point Z$'$). Hence, the decrease in the size of particle yields the increase in the solubility X_0^{cr} of components.

Note that, in contrast with the analysis for the cupola-shaped separation diagram of a bulk alloy, one needs to interpret the size-dependent separation diagram for a small particle in a different way. This is clear for the following reasons.

In fact, the usual cupola-shaped equilibrium diagram determines the solubility X_0^{cr} as well as the equilibrium concentrations ($X_{p,\infty} = X_0^{cr}$ and X_1) as a result of separation by one line (ASHPNF).

For a small particle the equilibrium diagram becomes doubled (and also shifted and size dependent). That is, instead of one line, one needs to deal with two lines, namely line MQZNL of solubility X_0^{cr} and line DQ$'$ENL of separation resulting in X_p^{opt} and X_1. It appears from this that the limiting solubility in a small particle does not coincide with the equilibrium concentration after the separation. We call this effect 'critical supersaturation'. (The notion of critical parameters with another
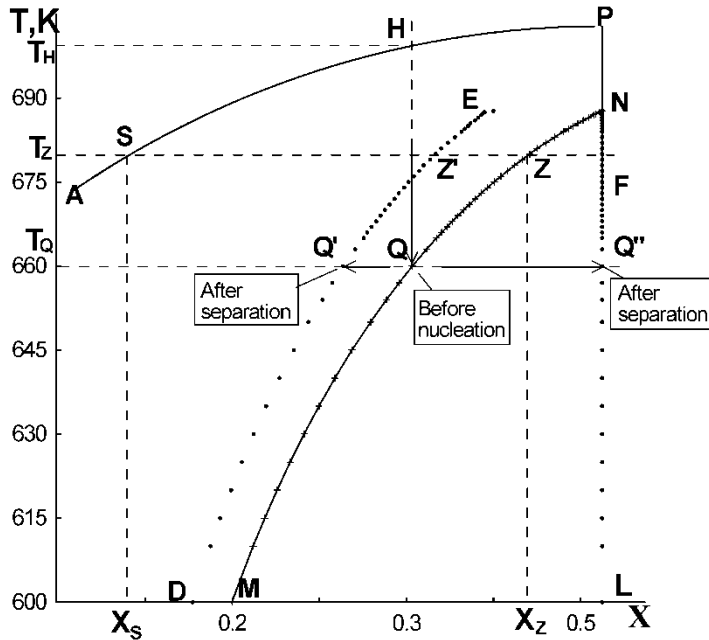
Figure 5. Size-dependent temperature–concentration state diagram. ASHPNF is the cupola-shaped diagram of a binary system for the case of separation in an infinite system, which is found analytically when the new phase is strictly stoichiometric; MQZNL is the cupola-shaped diagram of small particle at fixed radius R (the curve line connecting the experimental crosses is plotted for visualization of the cupola shape); the set of points $DQ'ENL$ determines the result of separation: X_p^{opt} (points $DQ'E$) and $X_1 = 0.5$ (points NL) in a small particle. The parameters are given in the main text.

choice of phase transition criterion was used by Ulbricht *et al.* (1988) and Schmelzer and Schweitzer (1990).) This means that separation is possible only (at some fixed temperature and size) if $\Delta X > \Delta X^{cr}$. Here $\Delta X^{cr} = X_0^{cr} - X_p^{opt}$ is the 'critical supersaturation', that is the difference between the limiting mean mole fraction of component B in the initially saturated alloy (or solubility concentration corresponding to the separation criterion) and optimal (or equilibrium) concentration in the parent phase *after* the separation. If the supersaturation ΔX is less than the 'critical supersaturation' ($\Delta X < \Delta X^{cr}$), which is a certain value for an alloy of fixed size R and temperature T, then nucleation and separation are impossible. The physical reason for this peculiarity consists of two factors. The first is a conservation law effect and the second is that the separation in a small particle may start only from nucleus formation, the volume of which is not small with respect to the total system volume.

It is clear from the present analysis and figure 5 that points Q', Q and Q'' correspond to the leverage rule $(N_{tot} - N_1) \Delta X^{cr} = N_1(X_1 - X_0^{cr})$, where N_1 is the total number of atoms in the new phase, N_{tot} is the total number of atoms in the binary system and the interval QQ' corresponds to ΔX^{cr}.

For a finite rate of T, R or X_0 changes, one should observe hysteresis behaviour (see below). Contrary to the usual hysteresis, which vanishes at infinitely slow processes ($dT/dt \rightarrow 0$ or $dR/dt \rightarrow 0$ or $dX_0/dt \rightarrow 0$), critical supersaturation does not disappear; as it is a thermodynamic characteristic depending on T and R
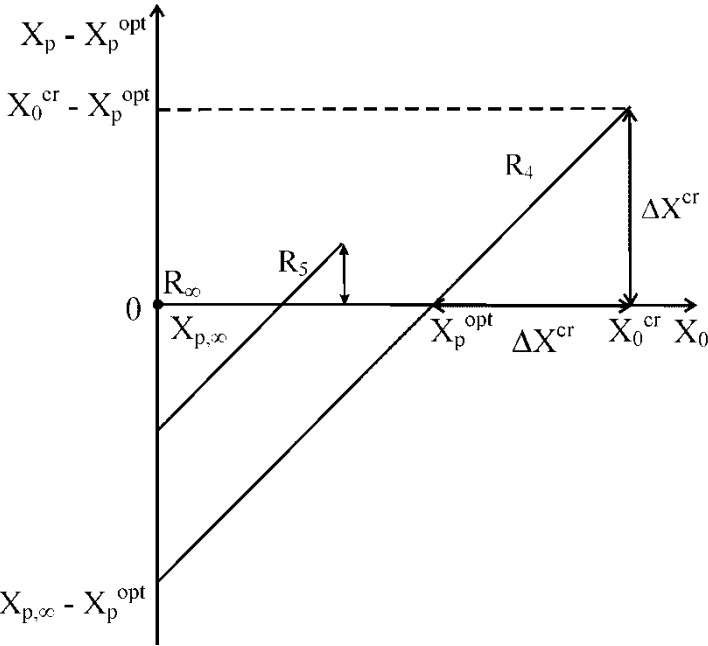
Figure 6.   Representation of the 'critical supersaturation' effect as a function of mean mole fraction X_0 of component B in the nanoalloy (note that X_p is a function of X_0, and X_p^{opt} is the size-dependent constant). The increase in supersaturation ends with an abrupt drop ΔX^{cr} after reading the separation criterion at $X_0 = X_0^{cr}$. Critical supersaturation depends on T and R. With increasing size the magnitude of the 'critical supersaturation' ΔX^{cr} decreases ($R_4 < R_5 < R_\infty = \infty$). The full square at the origin of the coordinate axes characterizes the zero value of 'critical supersaturation' in the case of separation in an infinite matrix (where $X_0^{cr} = X_p^{opt} = X_{p,\infty}$).

(figure 6). On increasing (decreasing) the size, the magnitude of the critical supersaturation ΔX^{cr} decreases (increases). In the limiting case of an infinite environment the 'critical supersaturation' ΔX^{cr} becomes zero.

The kinetic decoding of temperature hysteresis is presented qualitatively in figure 7 in which one hysteresis loop for concentration X_p is shown. (One can plot qualitatively similar diagrams for size hysteresis and concentration hysteresis.) Such hysteresis loops are typical for first-order phase transitions and characterize the finite rate of relaxation of the system to the minimum Gibbs free energy. The temperature hysteresis presented here is related to the existence of concentration depletion. The depletion is a parameter of the behaviour that makes the kinetic problem of behaviour of nanoalloys in a changing temperature field complicated. The 'kinetic decoding' of these transformations in the framework of a master equation approach is given in appendix A for a simplified model. Here, only general considerations are presented.

Hysteresis shows the irreversible character of state changes in the parent phase during cooling or heating at a finite speed. Line 10 represents the trend of the concentration curve in the parent phase from a supersaturated state (parent phase in figure 1(a)) at point 1 to a saturated state (parent phase in figure 1(a)) at point 0 (and vice versa) when a change in temperature does not change the concentration X_0 (i.e. the kinetic 'saturation' concentration). Curve 34 corresponds to the concentra-
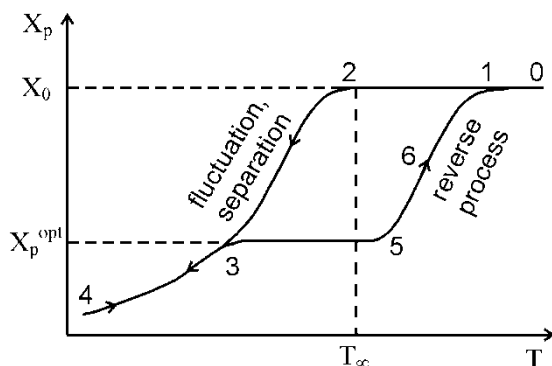
Figure 7. Qualitative representation of the 'hysteresis' effect in a nanosize particle: 012, supersaturated single-phase state (parent phase in figure 1(a)); 23, phase transition from the single-phase state at point 2 to the two-phase state (parent phase + phase 1 in figure 1(b)) at point 3; 34, 43, 35, cooled two-phase states (parent phase + phase 1); 561, phase transition from (parent phase + phase 1) state to single (parent phase) state. Point 2 approximately corresponds to point Q in figure 5; point 3 corresponds to point Q' in figure 5. The slope of the 23 interval depends on the cooling rate (and the 561 slope depends on the heating rate).

tion changes in X_p in the two-phase state (parent phase + new phase 1 in figure 1(b)) down to absolute depletion (depletion concentration at point 4). For the limiting case of infinite environment the asymptotic concentration will be determined by the value $X_{p,\infty}$. Thus during one circle the curve circumscribes a closed loop, namely a hysteresis loop. The form of the loop depends on the nature of substances and the rate of temperature or size change (similarly to internal friction in material under the cyclic deformation or magnetic induction of ferromagnetic in a changing external magnetic field).

The appearance of the hysteresis loop presented here is related to the nucleation barrier existence, non-monotonic and asymmetric $\Delta G(r)$ dependence curve (figure 3). Moreover, the $\Delta G(r)$ shape will lead to different fluctuation time values between the nucleation and separation and back transition (from a two-phase state to a single-phase state).

§6. CONCLUDING REMARKS

A thermodynamic model of decomposition in a binary nanoparticle is presented. A decomposition criterion for a small particle is reformulated.

In the description of the separation of a supersaturated solution in a small particle, one must distinguish the solubility limit (maximal impurity concentration before separation) and equilibrium concentration of the depleted parent phase after separation, the difference being called 'critical supersaturation'. The 'critical supersaturation' is a thermodynamic characteristic depending on the temperature and size.

For a finite rate of temperature, size and/or concentration changes, one should observe hysteresis behaviour.

The solubility in small particles increases even without taking into account interactions with the boundaries of the particle (if the density change is neglected). The general theory must take into account all three factors: external surface tension, interfacial tension and depletion of the parent phase by the new phase.

In our model we used several simplifications, some of which have been discussed in §2. Other limitations of the results presented are as follows.

(i) The intermediate phase is considered to be a line compound. The existence of a finite homogeneity range of the intermediate phase can be essential in the problem of reactive diffusion (when the diffusion flux and corresponding concentration gradient across the phase are necessary for reaction), but in our case of decomposition the small changes of composition inside the new phase can be neglected.

(ii) The concentration distribution in the particle was considered as step like at each moment of decomposition. This model can be modified in the framework of the Cahn–Hilliard (1959) approach with gradient terms in the density of Gibbs energy leading to a diffuse interface. However, this modification (much more complicated in a mathematical sense) leads qualitatively to the same results (for example Shirinyan and Gusak (1999)).

(iii) Segregation effects have been neglected. Segregation can be important for equilibrium redistribution (Weissmuller and Ehrhardt 1998). The influence of this aspect on the splitting of equilibrium curves and hysteresis will be analysed elsewhere.

(iv) The size and shape of the whole system remained constant, so that the contribution of external surface tension did not play any role. Geometrical effects may be introduced in the framework of the presented analysis using the recent results for the modelling of shape-dependent phase diagrams of nanoparticles (Wautelet *et al.* 2003).

The offered model may be generalized for the analysis of the phase diagrams in the case of competitive nucleation and growth of two (or many) intermediate phases in volumes of nanometric size (Shirinyan *et al.* 2000).

APPENDIX A

HYSTERESIS OF PHASE SEPARATION IN AN ENSEMBLE
OF SMALL ISOLATED PARTICLES

Here we present a numerical analysis of hysteresis in an ensemble of isolated nanoparticles, using the standard kinetic master equation approach. (The calculations in this appendix have been made in collaboration with Mykola Pasichny.) When such a system is quenched into the two-phase region, separation proceeds via nucleation and growth of the new phase nuclei. Here we solve the problem of unsteady-state nucleation kinetics when taking into account the time- and size-dependent depletion. In our case the Gibbs free energy (4) is a function of time (via the time-dependent temperature).

To carry out the subsequent analysis we introduce a size distribution function $f(\tilde{N}, t)$, that is the number of droplets of the new phase consisting of $\tilde{N}$ structure units AB at moment t. As was mentioned above, $X_0 < 0.5$, $X_1 > X_0$ and $X_1 = 0.5$; so the number $\tilde{N}$ of units in each nucleus coincides with the number of atoms of B type: $\tilde{N} = N_B$ and $f(\tilde{N}, t) = f(N_B, t)$. The process is controlled by the mobility of component B. Moreover, at each moment, both phases are treated as homogeneous.

The evolution of an ensemble of clusters formed by the nucleation and growth processes will be described by the master equation

$$\frac{\partial f(N_B, t)}{\partial t} = f(N_B - 1, t)v_+(N_B - 1) + f(N_B + 1, t)v_-(N_B + 1)$$
$$- f(N_B, t)\big[v_-(N_B) + v_+(N_B)\big]. \tag{A 1}$$

The frequency $v_+(N_B)$ of attachment and the frequency $v_-(N_B)$ of detachment of monomer AB to a cluster of size N_B are interrelated as usual:

$$v_-(N_B) = v_+(N_B) \exp\left(\frac{\Delta G(N_B) - \Delta G(N_B - 1)}{kT}\right). \tag{A 2}$$

The change $\Delta G(N_B)$ in the free energy per particle is determined by equation (4) and may be rewritten as

$$\Delta G(N_B) = \Delta g_1(T)\frac{N_B}{X_1} + \Delta g_0\big(T, X_p(N_B)\big)\left(N_{\text{tot}} - \frac{N_B}{X_1}\right)$$
$$- \Delta g_0(T, X_0)\, N_{\text{tot}} + \frac{3}{2}B\left(\frac{N_B}{X_1}\right)^{2/3}, \tag{A 3}$$

where again N_{tot} is the total number of atoms in one particle ($N_{\text{tot}} = 4\pi R^3 n/3$) and $B = 2(4\pi/3)^{1/3}(\sigma/n^{2/3})$ is the coefficient of the surface energy contribution.

The mole fraction X_p in the depleted parent phase is a function of the number N_B of units:

$$X_p(N_B) = \frac{X_0 N_{\text{tot}} - N_B}{N_{\text{tot}} - N_B/X_1}. \tag{A 4}$$

Further $v_+(N_B)$ will be taken as constant; so we use a variable for time: $\tau = v_+ t$.

The cluster size distribution function $f(N_B, \tau)$ obeys the boundary condition, which is reduced simply to the conservation of particles:

$$f(N_0, \tau) = W - \sum_{N_B = N_0 + 1} f(N_B, \tau). \tag{A 5}$$

W is the total number of isolated nanoparticles in the ensemble coinciding with the number of nuclei (one nucleus in one particle) and N_0 is the minimal number of building units in the nuclei.

The initial conditions are

$$f(N_B, \tau = 0) = \begin{cases} W, & N_B = N_0, \\ 0, & N_B \neq N_0. \end{cases} \tag{A 6}$$

The aim of this model is to trace the average composition of the depleted parent phase during the temperature cycling of the ensemble of isolated nanoparticles.
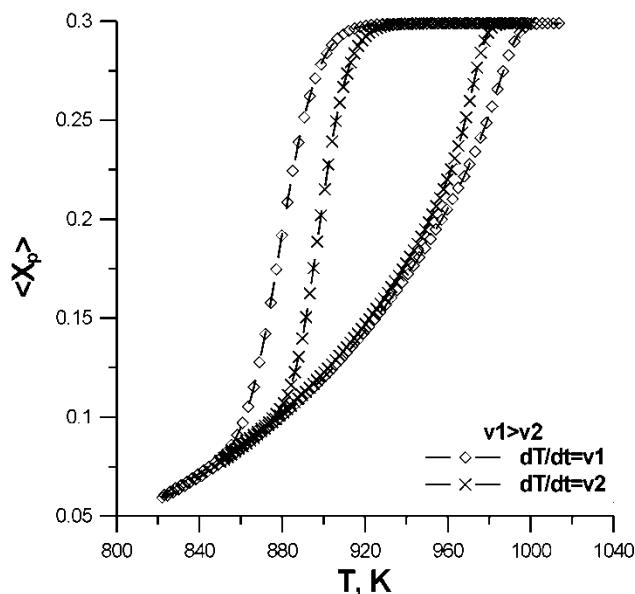
Figure A1.   Evolution of the mean concentration in the parent phase of an ensemble of isolated nanoparticles: dependence of the average concentration $\langle X_p \rangle$ on temperature T for two different constant rates of temperature changes $\upsilon = dT/d\tau$ with time where $\upsilon_1 > \upsilon_2$; ($\diamond$), $\upsilon_1 = 0.03$ K; ($\times$), $\upsilon_2 = 0.01$ K.

This concentration is determined by the formula

$$\langle X_p \rangle = \frac{\sum_{N_B = N_0} f(N_B, \tau) X_p(N_B)}{\sum_{N_B = N_0} f(N_B, \tau)}. \qquad (A\,7)$$

Numerical calculations have been realized for the following set of parameters: $X_0 = 0.3$; $X_1 = 0.5$; $N_{tot} = 1000$; $N_0 = 2$; $W = 10^{10}$; $\Delta g_1 = -4.5 \times 10^{-20}$ J; $\alpha = 2.3$; $B = 2 \times 10^{-20}$ J. The detailed analysis will be discussed elsewhere. Here we shall show only the evolution of the mean concentration $\langle X_p \rangle$ in the process of temperature cycling from a high temperature T_1 to a low temperature T_3 (see figure 3 (a)) and back for different rates $\upsilon = dT/d\tau$ of temperature changes (figure A 1).

REFERENCES

CAHN, J. W., and HILLIARD, J. E., 1959, *J. chem. Phys.*, **31**, 688.
CHEN, S.-W., JAN, C.-H., LIN, J.-C., and CHANG, A., 1989, *Metall. Trans. A.*, **20**, 2247.
CHIGHIK, S. P., GLADGKIKH, M. T., GRIGORIJEVA, L. K., KUKLIN, R. N., STEPANOVA, S. V., and CHMEL, S. V., 1985, *Izv. Akad. Nauk USSR*, (2), 175.
CHRISTIAN, J. W., 1965, *Theory of Transformation in Metals and Alloys* (Oxford: Pergamon).
DENBIGH, P. N., and MARCUS, R. B., 1966, *J. appl. Phys.*, **37**, 4325.
GLADGKIKH, M. T., CHIGIK, S. P., LARIN, V. N., GRIGORIJEVA, L. K., and SUHOV, V. N., 1988, *Dokl. Akad. Nauk USSR*, **300**, 588.
GUSAK, A. M., and SHIRINYAN, A. S., 1998, *Metal Phys. Adv. Technol.*, **20**, 40.
HUTCHINSON, T. E., 1963, *Appl. Phys. Lett.*, **3**, 51.
LIFSHITS, I. M., and SLEZOV, V. V., 1961, *J. Phys. Chem. Solids*, **19**, 35.
LUDWIG, F. P., and SCHMELZER, J., 1996, *J. Colloid Interface Sci.*, **181**, 503.
MOORE, K. L., CHATTOPADHYAY, K., and CANTOR, B., 1987, *Proc. R. Soc.* A, **414**, 499.
NAGAEV, E. L., 1992, *Usp. Fiz. Nauk*, **162**, 50.
PALATNIK, L. S., and COMNIK, J. F., 1960, *Fiz. Magn. Mater.*, **9**, 374.

PETROV, Y. I., 1982, *Physics of Small Particles* (Moscow: Science).

RUSANOV, A. I., 1967, *Phase Equilibria and Surface Phenomena* (Leningrad: Chemistry).

SAUNDERS, N., 1977, Calphad, **3**, 237.

SHIRINYAN, A. S., 2000, PhD Thesis, Cherkasy State University, Cherkasy, Ukraine.

SHIRINYAN, A. S., and GUSAK, A. M., 1999, *Ukr. Fiz. J.*, **44**, 883.

SHIRINYAN, A. S., GUSAK, A. M., and DESRE, P. J., 2000, *J. metastable nanocrystalline Mater.*, **7**, 17.

SCHMELZER, J., and SCHWEITZER, F., 1990, *Z. phys. Chem.*, **271**, 565.

ULBRICHT, H., SCHMELZER, J., MAHNKE, R., and SCHWEITZER, F., 1988, *Thermodynamics of Finite Systems and Kinetics of First-Order Phase Transitions* (Leipzig: BSB Teubner).

WAGNER, C., 1961, *Z. Electrochem.*, **65**, 581.

WAUTELET, M., 1991, *J. Phys. D*, **24**, 343; 2000, *Nanotechnology*, **11**, 6.

WAUTELET, M., DAUCHOT, J. P., and HECQ, M., 2003, *J. Phys.: condens. Matter*, **15**, 3651.

WEISSMULLER, J., and EHRHARDT, H., 1998, *Phys. Rev. Lett.*, **81**, 1114.